

Interaction of two optical vortices propagating through turbulent atmosphere

Penghui Ga(高鹏慧), Chaona Bian(边超娜), Meihong Lu(逯美红), Jinlu Li(李金录), Yiling He(贺艺玲), Jingying Li(李京英)

Citation: Chin. Phys. B. 35, 094214 (2026). DOI: 10.1088/1674-1056/ae31dc |
CSTR: 32038.14.CPB.ae31dc
http://cpb.iphy.ac.cn; http://iopscience.iop.org/cpb

What follows is a list of articles you may be interested in

Distorted dislocations and OAM spectra of twisted partially coherent noncanonical vortex-pair beams in non-Kolmogorov atmospheric turbulence

Chao Mei(梅超), Ke Cheng(程科), Hao Guo(郭豪), Xiao-Wen Yi(易小雯)
Chin. Phys. B. 35, 064207 (2026). DOI: 10.1088/1674-1056/ae07c1 | CSTR: 32038.14.CPB.ae07c1

Continuous three-dimensional varifocal of vortex beams with twisted metasurfaces

Yiyi Li(黎仪艺), Wangzhe Zhou(周王哲), Shaoqi Li(李少奇), Xiaoyan Huang(黄晓艳), Fen Zhao(赵芬), Man Yuan(袁满), Jiagui Wu(吴加贵), Huan Chen(陈欢), Zhaojian Zhang(张兆健), Junbo Yang(杨俊波)
Chin. Phys. B. 35, 034208 (2026). DOI: 10.1088/1674-1056/adfc42 | CSTR: 32038.14.CPB.adfc42

Fusion of fractional vortex pairs and their transition to integer vortex controlled by optical power

Chunzhi Sun(孙春志), Xiangwei Chen(陈向炜), Huizhong Xu, Guo Liang(梁果)
Chin. Phys. B. 34, 054202 (2025). DOI: 10.1088/1674-1056/adb8b9 | CSTR: 32038.14.CPB.adb8b9

Modulation of Bessel-like vector vortex beam using the resonant magneto-optical effect in rubidium vapor

Yan Ma(马燕), Xin Yang(杨欣), Hong Chang(常虹), Ming-Tao Cao(曹明涛), Xiao-Fei Zhang(张晓斐), Rui-Fang Dong(董瑞芳), Shou-Gang Zhang(张首刚)
Chin. Phys. B. 34, 024202 (2025). DOI: 10.1088/1674-1056/ad9c43 | CSTR: 32038.14.CPB.ad9c43

Optimization of extreme ultraviolet vortex beam based on high harmonic generation

Bo Xiao(肖礴), Yi-Wen Zhao(赵逸文), Fang-Jing Cheng(程方晶), Ge-Wen Wang(王革文), Wei Jiang(姜威), Yi-Chen Wang(王一琛), Jie Hu(胡杰), Hong-Jing Liang(梁红静), Ri Ma(马日)
Chin. Phys. B. 33, 054209 (2024). DOI: 10.1088/1674-1056/ad2bf0

Interaction of two optical vortices propagating through turbulent atmosphere

Penghui Gao(高鹏慧)[1,3,†], Chaona Bian(边超娜)[1], Meihong Lu(逯美红)[1], Jinlu Li(李金录)[2], Yiling He(贺艺玲)[1], and Jingying Li(李京英)[4]

[1]*Department of Physics, Changzhi University, Changzhi* 046011, *China*
[2]*School of Physics, Xidian University, Xi'an* 710071, *China*
[3]*Laboratory of Optical Field Manipulations, Department Of Physics, Changzhi University, Changzhi* 046011, *China*
[4]*School of Communications and Information Engineering, Xi'an University of Posts and Telecommunications, Xi'an* 710061, *China*

(Received 21 November 2025; revised manuscript received 24 December 2025; accepted manuscript online 30 December 2025)

Optical vortices are associated with orbital angular momentum (OAM) and play a significant role in optical communications. During propagation through turbulent atmosphere, optical vortices are subject to atmospheric turbulence, which induces effects such as vortex annihilation. This paper investigates the interaction of two optical vortices during their propagation through turbulent atmosphere. The results show that when the topological charge magnitudes of the two optical vortices are m and n, they evolve into $m+n$ optical vortices, each with a topological charge magnitude of 1. As the propagation distance increases: when the topological charges of the two optical vortices have equal magnitudes but opposite signs, the wavefront exhibits either no optical vortex or a pair of optical vortices with topological charges of ±1 after sufficiently long propagation; when the topological charges have unequal magnitudes and opposite signs, the wavefront contains $m+n$, $m+n-2$, or $|m-n|$ optical vortices after sufficiently long propagation. These findings can provide theoretical guidance for the control of optical vortex propagation.

Keywords: optical vortex, turbulent atmosphere, topological charge, orbital angular momentum (OAM)

PACS: 47.32.C–, 42.68.Bz, 03.65.Vf, 42.50.Tx

DOI: 10.1088/1674-1056/ae31dc **CSTR:** 32038.14.CPB.ae31dc

1. Introduction

Singular optics is an emerging branch of modern optics, primarily focusing on phase singularities in light waves and the topological structure of wavefronts.[1] Optical vortices represent a specific manifestation of phase singularities in light waves and are intrinsically linked to OAM.[2] At the core of an optical vortex, the phase remains indeterminate, with the intensity equaling zero.[3] Owing to its profound theoretical significance[4,5] and wide-ranging applications in optical communications,[6,7] optical micromanipulation,[8–10] optical data storage,[11,12] and quantum cryptography,[13,14] this field has attracted extensive research interest.

Chen *et al.* pointed out that optical vortices offer distinctive advantages for information encoding, particularly suitable for high-capacity optical communications, and identified mode modulation/demodulation, mode processing, and mode transmission as the three pillars of optical vortex communication networks.[15] Zhang *et al.* proposed a mechanism for generating optical spatiotemporal vortex pulses with fixed central frequency and momentum, which they subsequently verified experimentally.[16] Chen *et al.* developed a novel nanoscale vortex generation strategy that achieves precise control over the intensity and phase of transmitted light by manipulating the coupling of adjacent nanopillars, enabling the efficient nanoscale generation of vortex beams carrying different topological charges.[17] Jo *et al.* reported that spin–orbit coupling in van der Waals materials can give rise to optical vortices, demonstrating that an 8-μm-thick hexagonal boron nitride crystal can produce optical vortices with topological charges of ±2.[18] Peters *et al.* systematically expounded a digital approach to the transmission of structured light in turbulent atmosphere.[19] Li *et al.* experimentally generated vector vortex pin-like beams and numerically simulated their propagation through turbulent atmosphere, showing that such beams exhibit significant advantages in mitigating turbulence effects.[20] Gao *et al.* studied the spiral spectrum and channel capacity of a Gaussian beam carrying a fractional-order optical vortex and an edge dislocation during propagation in turbulent atmosphere, revealing the relationship between wavefront phase distribution and OAM modes.[21] Saad *et al.* examined the influence of turbulent atmosphere on the propagation characteristics of modified anomalous vortex beams.[22] Bai *et al.* reported a new type of vortex beam and analyzed its channel capacity and bit error rate in propagation through turbulent atmosphere.[23] Duan *et al.*, based on the Young's double-slit interference principle and using vortex beams as the coherent light source, investigated the relationship between interference patterns and topological charges.[24] Gao *et al.* explored the

†Corresponding author. E-mail: penghgao@163.com

© 2026 Chinese Physical Society and IOP Publishing Ltd. All rights, including for text and data mining, AI training, and similar technologies, are reserved.

influence of edge dislocation on optical vortex propagation and found that, in free space, the presence of an edge dislocation renders higher-order optical vortices unstable, causing them to evolve into two optical vortices.[25] Lyu *et al.* designed a polarized optical multi-vortex generator.[26] We will investigate the propagation characteristics of two optical vortices, and explore the interaction between the two optical vortices under the influence of turbulence perturbations in turbulent atmosphere. The research conclusions will provide a theoretical basis for the propagation control of optical vortices.

Therefore, the objective of this paper is to conduct a detailed investigation into the evolution of two optical vortices propagating through turbulent atmosphere. Section 2 presents the field expression of a Gaussian beam carrying two optical vortices at the source plane and derives the analytical expression of its cross-spectral density function during propagation in turbulent atmosphere. Section 3 analyzes the propagation of two noncanonical optical vortices with opposite topological charge signs in turbulent atmosphere. Section 4 examines the propagation of two canonical optical vortices with opposite topological charge signs in turbulent atmosphere. Section 5 discusses the case of two optical vortices with identical topological charge signs. Finally, this paper provides a summary of the main findings of the study.

2. Propagation model

At point $(p_x,\ p_y)$ in a rectangular coordinate system, an isolated n-fold degenerate intensity null can be expressed as

$$T(x,y) = [a(x-p_x) + \mathrm{i}(y-p_y)]^q, \tag{1}$$

where a is a dimensionless parameter associated with the sign of the optical vortex's topological charge and its phase distribution, and q denotes the magnitude of the topological charge. The sign and magnitude of an optical vortex's topological charge are governed by the sign convention:[27] when the phase increases in the counterclockwise direction, the topological charge sign is positive ("+"); otherwise, the topological charge sign is negative ("−"). For an optical vortex with topological charge magnitude of l, the phase changes (increases) by $2l\pi$. The topological charge of the optical vortex is represented by the combination of its sign and magnitude.[27]

By embedding intensity nulls at $(b,\ 0)$ and $(-d,\ 0)$ into a Gaussian beam using Eq. (1), the field expression of a Gaussian beam carrying two optical vortices at the source plane can be written as

$$E_0(\boldsymbol{s}, z=0) = \frac{[a(s_x-b)+\mathrm{i}s_y]^n\,[c(s_x+d)+\mathrm{i}s_y]^m}{w_0^{n+m}} \times \exp\left(-\frac{s_x^2+s_y^2}{w_0^2}\right), \tag{2}$$

where $\boldsymbol{s} = (s_x, s_y)$ is a two-dimensional plane vector, w_0 is the beam waist width, and c, like a, is a dimensionless parameter related to the phase distribution and the sign of the optical vortex's topological charge. m and n denote the magnitudes of the two optical vortices' topological charges, respectively.

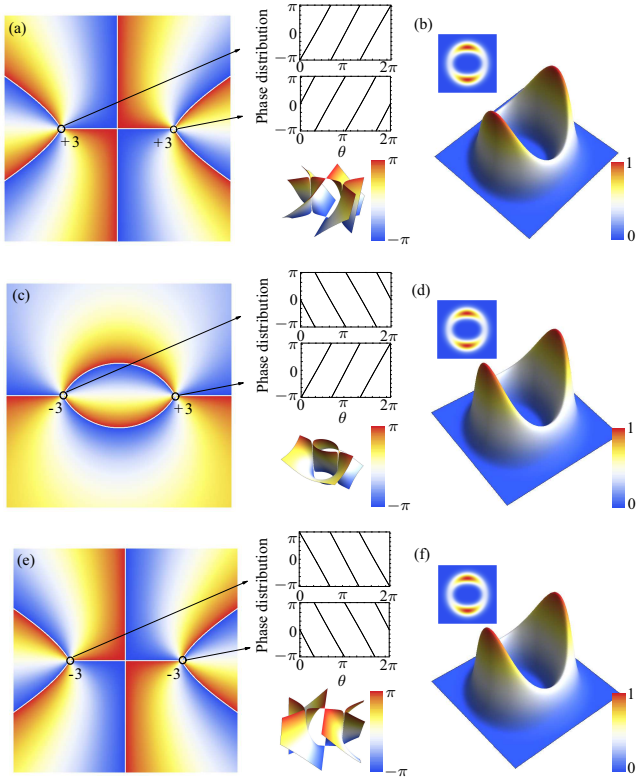


Fig. 1. Phase distributions (a), (c), (e) and normalized intensity distributions (b), (d), (f) of a Gaussian beam carrying two optical vortices at the source plane. $a = 1$, $c = 1$ (a), (b); $a = 1$, $c = -1$ (c), (d); and $a = -1$, $c = -1$ (e), (f).

Based on Eq. (2), Figs. 1 and 2 illustrate the phase and normalized intensity distributions at the source plane for a Gaussian beam carrying two optical vortices. The calculation parameters for Fig. 1 are $w_0 = 2$ cm, $a = 1$, $c = 1$ (a), (b), $a = 1$, $c = -1$ (c), (d), $a = -1$, $c = -1$ (e), (f), $b = 1$ cm, $d = 1$ cm, $n = 3$, and $m = 3$. The parameters for Fig. 2 are $a = 2$, $c = 2$ (a), (b), $a = 2$, $c = -2$ (c), (d), and $a = -2$, $c = -2$ (e), (f), with other parameters identical to those in Fig. 1. According to Figs. 1(a), 1(b) and 2(a), 2(b), there exist two optical vortices with identical topological charges of $+3$ at the source plane. Figures 1(c), 1(d) and 2(c), 2(d) show two optical vortices with topological charges of $+3$ and -3, respectively. Figures 1(e), 1(f) and 2(e), 2(f) indicate two optical vortices both carrying topological charges of -3 at the source plane. It is also evident from Figs. 1 and 2 that when $a = \pm 1$ or $c = \pm 1$, the phase increment of the optical vortex varies linearly, whereas for $a = \pm 2$ or $c = \pm 2$, the phase increment is nonlinear. Therefore, the optical vortices in Figs. 1 and 2 correspond to canonical and noncanonical optical vortices, respectively. The physical distinction between noncanonical

optical vortices and canonical optical vortices lies in the number of OAM modes they correspond to. Canonical optical vortices correspond to one OAM mode, while noncanonical optical vortices correspond to multiple OAM modes.[28,29] The "multi-modes superposition" breaks the symmetric intensity distribution of canonical optical vortices, causing the intensity profile to deviate from the doughnut shape and exhibit more complex characteristics.[30,31] This also explains why the intensity distribution in Fig. 2 differs from that in Fig. 1. The research can further promote the development of light intensity modulation technology.

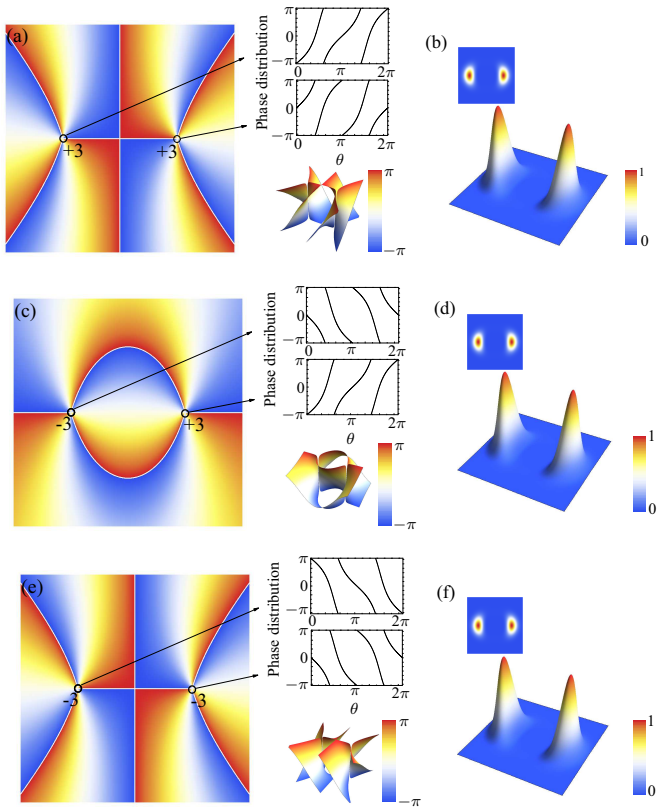


Fig. 2. Phase distributions (a), (c), (e) and normalized intensity distributions (b), (d), (f) of a Gaussian beam carrying two optical vortices at the source plane. $a=2$, $c=2$ (a), (b); $a=2$, $c=-2$ (c), (d); and $a=-2$, $c=-2$ (e), (f).

By employing the following equation:[32]

$$(px+\mathrm{i}y)^q=\sum_{l=0}^{q}\frac{q!}{l!\,(q-l)!}(px)^l(\mathrm{i}y)^{q-l}, \tag{3}$$

Eq. (2) can be rewritten as

$$\begin{aligned}E_0(s_x,s_y,z=0)=&\sum_{l=0}^{n}\frac{n!a^l\mathrm{i}^{n-l}}{l!\,(n-l)!}\sum_{e=0}^{l}\frac{l!\,(-b)^{l-e}}{e!\,(l-e)!}\\&\times\sum_{r=0}^{m}\frac{m!c^r\mathrm{i}^{m-r}}{r!\,(m-r)!}\sum_{f=0}^{r}\frac{r!\,(d)^{r-f}}{f!\,(r-f)!}\\&\times\frac{s_x^{e+f}s_y^{n-l+m-r}}{w_0^{n+m}}\exp\left(-\frac{s_x^2+s_y^2}{w_0^2}\right).\end{aligned} \tag{4}$$

The analytical expression for the cross-spectral density function of a Gaussian beam carrying two optical vortices at the source plane ($z=0$) is given by

$$\begin{aligned}&W_0(\boldsymbol{s}_1,\boldsymbol{s}_2,z=0)\\&=\langle E_{01}^*(\boldsymbol{s}_1,z=0)E_{02}(\boldsymbol{s}_2,z=0)\rangle\\&=\sum_{l_1=0}^{n}\frac{n!a^{l_1}(-\mathrm{i})^{n-l_1}}{l_1!\,(n-l_1)!}\sum_{e_1=0}^{l_1}\frac{l_1!\,(-b)^{l_1-e_1}}{e_1!\,(l_1-e_1)!}\\&\times\sum_{r_1=0}^{m}\frac{m!c^{r_1}(-\mathrm{i})^{m-r_1}}{r_1!\,(m-r_1)!}\sum_{f_1=0}^{r_1}\frac{r_1!\,(d)^{r_1-f_1}}{f_1!\,(r_1-f_1)!}\\&\times\sum_{l_2=0}^{n}\frac{n!a^{l_2}\mathrm{i}^{n-l_2}}{l_2!\,(n-l_2)!}\sum_{e_2=0}^{l_2}\frac{l_2!\,(-b)^{l_2-e_2}}{e_2!\,(l_2-e_2)!}\\&\times\sum_{r_2=0}^{m}\frac{m!c^{r_2}\mathrm{i}^{m-r_2}}{r_2!\,(m-r_2)!}\sum_{f_2=0}^{r_2}\frac{r_2!\,(d)^{r_2-f_2}}{f_2!\,(r_2-f_2)!}\\&\times\frac{s_{1x}^{e_1+f_1}s_{1y}^{n-l_1+m-r_1}s_{2x}^{e_2+f_2}s_{2y}^{n-l_2+m-r_2}}{w_0^{2(n+m)}}\\&\times\exp\left(\frac{-s_{1x}^2-s_{1y}^2-s_{2x}^2-s_{2y}^2}{w_0^2}\right).\end{aligned} \tag{5}$$

According to the generalized Huygens–Fresnel principle,[33] the cross-spectral density function of a Gaussian beam carrying two optical vortices propagating through turbulent atmosphere can be expressed as

$$\begin{aligned}W(\boldsymbol{\rho}_1,\boldsymbol{\rho}_2,z)=&\left(\frac{k}{2\pi z}\right)^2\int\int\int\int W_0(\boldsymbol{s}_1,\boldsymbol{s}_2,z=0)\\&\times\exp\left\{-\frac{\mathrm{i}k}{2z}\left[(\boldsymbol{s}_1-\boldsymbol{\rho}_1)^2-(\boldsymbol{s}_2-\boldsymbol{\rho}_2)^2\right]\right\}\\&\times\langle\exp\left[\varphi^*(\boldsymbol{\rho}_1,\boldsymbol{s}_1)+\varphi(\boldsymbol{\rho}_2,\boldsymbol{s}_2)\right]\rangle\,\mathrm{d}\boldsymbol{s}_1\,\mathrm{d}\boldsymbol{s}_2,\end{aligned} \tag{6}$$

where $\boldsymbol{\rho}_1=(\rho_{1x},\rho_{1y})$ and $\boldsymbol{\rho}_2=(\rho_{2x},\ \rho_{2y})$ are the position coordinates of two points on the output plane, k is the wave number defined by $k=2\pi/\lambda$, and $\langle\cdot\rangle$ denotes the phase fluctuations induced by turbulence. These fluctuations can be approximated as[34]

$$\begin{aligned}&\langle\exp\left[\varphi^*(\boldsymbol{\rho}_1,\boldsymbol{s}_1)+\varphi(\boldsymbol{\rho}_2,\boldsymbol{s}_2)\right]\rangle\\&\approx\exp\left[-\frac{(\boldsymbol{s}_1-\boldsymbol{s}_2)^2+(\boldsymbol{\rho}_1-\boldsymbol{\rho}_2)^2+(\boldsymbol{s}_1-\boldsymbol{s}_2)(\boldsymbol{\rho}_1-\boldsymbol{\rho}_2)}{\rho_0^2}\right],\end{aligned} \tag{7}$$

where $\rho_0=\left(0.545C_n^2k^2z\right)^{-3/5}$ represents the correlation length of a spherical wave propagating through turbulent atmosphere, and C_n^2 is the refractive index structure constant. A larger value of C_n^2 corresponds to stronger atmospheric turbulence.

By employing the following equation:[32]

$$\begin{aligned}&\int x^n\exp\left(-px^2+2qx\right)\mathrm{d}x\\&=n!\exp\left(\frac{q^2}{p}\right)\sqrt{\frac{\pi}{p}}\left(\frac{q}{p}\right)^n\\&\times\sum_{k=0}^{E\left[\frac{n}{2}\right]}\frac{1}{(n-2k)!k!}\left(\frac{p}{4q^2}\right)^k,\quad(n=0,1,2,\ldots)\end{aligned} \tag{8}$$

and performing the integration, the analytical expression for the cross-spectral density function of a Gaussian beam carrying two optical vortices propagating through turbulent atmosphere is obtained as follows:

$$\begin{aligned} W(\boldsymbol{\rho}_1,\boldsymbol{\rho}_2,z) = & \sum_{l_1=0}^{n} \frac{n!a^{l_1}(-\mathrm{i})^{n-l_1}}{l_1!(n-l_1)!} \sum_{e_1=0}^{l_1} \frac{l_1!(-b)^{l_1-e_1}}{e_1!(l_1-e_1)!} \sum_{r_1=0}^{m} \frac{m!c^{r_1}(-\mathrm{i})^{m-r_1}}{r_1!(m-r_1)!} \sum_{f_1=0}^{r_1} \frac{r_1!(d)^{r_1-f_1}}{f_1!(r_1-f_1)!w_0^{2(n+m)}} \\ & \times \sum_{l_2=0}^{n} \frac{n!a^{l_2}\mathrm{i}^{n-l_2}}{l_2!(n-l_2)!} \sum_{e_2=0}^{l_2} \frac{l_2!(-b)^{l_2-e_2}}{e_2!(l_2-e_2)!} \sum_{r_2=0}^{m} \frac{m!c^{r_2}\mathrm{i}^{m-r_2}}{r_2!(m-r_2)!} \sum_{f_2=0}^{r_2} \frac{r_2!(d)^{r_2-f_2}k^2C_1C_2}{f_2!(r_2-f_2)!4\pi^2z^2} \\ & \times \exp\left[-\frac{(\rho_{1x}-\rho_{2x})^2+(\rho_{1y}-\rho_{2y})^2}{\rho_0^2} - \frac{\mathrm{i}k}{2z}\left(\rho_{1x}^2+\rho_{1y}^2-\rho_{2x}^2-\rho_{2y}^2\right)\right] C_3C_4, \end{aligned} \tag{9}$$

where

$$C_1 = \frac{(e_1+f_1)!}{A_1^{e_1+f_1}} \exp\left(\frac{B_1^2}{A_1}\right) \sqrt{\frac{\pi}{A_1}} \sum_{h_1=0}^{E\left[\frac{e_1+f_1}{2}\right]} \frac{A_1^{h_1}}{4^{h_1}(e_1+f_1-2h_1)!h_1!} \sum_{s_1=0}^{e_1+f_1-2h_1} \frac{(e_1+f_1-2h_1)!B_1^{s_1}}{s_1!(e_1+f_1-2h_1-s_1)!} \left(\frac{1}{\rho_0^2}\right)^{e_1+f_1-2h_1-s_1}, \tag{10}$$

$$\begin{aligned} C_2 = & \frac{(e_2+f_2+e_1+f_1-2h_1-s_1)!B_2^{e_2+f_2+e_1+f_1-2h_1-s_1}}{A_2^{e_2+f_2+e_1+f_1-2h_1-s_1}} \exp\left(\frac{B_2^2}{A_2}\right)\sqrt{\frac{\pi}{A_2}} \\ & \times \sum_{h_2=0}^{E\left[\frac{e_2+f_2+e_1+f_1-2h_1-s_1}{2}\right]} \frac{A_2^{h_2}}{4^{h_2}B_2^{2h_2}(e_2+f_2+e_1+f_1-2h_1-s_1-2h_2)!h_2!}, \end{aligned} \tag{11}$$

$$\begin{aligned} C_3 = & \frac{(n-l_1+m-r_1)!}{A_1^{n-l_1+m-r_1}} \exp\left(\frac{B_3^2}{A_1}\right)\sqrt{\frac{\pi}{A_1}} \sum_{h_3=0}^{E\left[\frac{n-l_1+m-r_1}{2}\right]} \frac{A_1^{h_3}}{4^{h_3}(n-l_1+m-r_1-2h_3)!h_3!} \\ & \times \sum_{s_2=0}^{n-l_1+m-r_1-2h_3} \frac{(n-l_1+m-r_1-2h_3)!B_3^{s_2}}{s_2!(n-l_1+m-r_1-2h_3-s_2)!} \left(\frac{1}{\rho_0^2}\right)^{n-l_1+m-r_1-2h_3-s_2}, \end{aligned} \tag{12}$$

$$\begin{aligned} C_4 = & \frac{(n-l_2+m-r_2+n-l_1+m-r_1-2h_3-s_2)!B_4^{n-l_2+m-r_2+n-l_1+m-r_1-2h_3-s_2}\sqrt{\pi}}{A_2^{n-l_2+m-r_2+n-l_1+m-r_1-2h_3-s_2}\sqrt{A_2}} \exp\left(\frac{B_4^2}{A_2}\right) \\ & \times \sum_{h_4=0}^{E\left[\frac{n-l_2+m-r_2+n-l_1+m-r_1-2h_3-s_2}{2}\right]} \frac{(0.25A_2)^{h_4}}{B_4^{2h_4}(n-l_2+m-r_2+n-l_1+m-r_1-2h_3-s_2-2h_4)!h_4!}. \end{aligned} \tag{13}$$

In C_1, C_2, C_3, and C_4, the expressions of A_1, A_2, B_1, B_2, B_3, and B_4 are as follows:

$$A_1 = \frac{1}{w_0^2} + \frac{\mathrm{i}k}{2z} + \frac{1}{\rho_0^2}, \quad A_2 = \frac{1}{w_0^2} - \frac{\mathrm{i}k}{2z} + \frac{1}{\rho_0^2} - \frac{1}{A_1\rho_0^4}, \tag{14}$$

$$B_1 = \frac{\mathrm{i}k\rho_{1x}}{2z} - \frac{(\rho_{1x}-\rho_{2x})}{2\rho_0^2},$$

$$B_2 = \frac{B_1}{A_1\rho_0^2} - \frac{\mathrm{i}k\rho_{2x}}{2z} + \frac{\rho_{1x}-\rho_{2x}}{2\rho_0^2}, \tag{15}$$

$$B_3 = \frac{\mathrm{i}k\rho_{1y}}{2z} - \frac{(\rho_{1y}-\rho_{2y})}{2\rho_0^2},$$

$$B_4 = \frac{B_3}{A_1\rho_0^2} - \frac{\mathrm{i}k\rho_{2y}}{2z} + \frac{\rho_{1y}-\rho_{2y}}{2\rho_0^2}. \tag{16}$$

According to the definition of spectral degree of coherence,[35]

$$\mu(\boldsymbol{\rho}_1,\boldsymbol{\rho}_2,z) = \frac{W(\boldsymbol{\rho}_1,\boldsymbol{\rho}_2,z)}{[I(\boldsymbol{\rho}_1,z)I(\boldsymbol{\rho}_2,z)]^{1/2}}, \tag{17}$$

where $I(\boldsymbol{\rho}_i,z) = W(\boldsymbol{\rho}_i,\boldsymbol{\rho}_i,z)$ $(i = 1, 2)$ represents the optical intensity at point $(\boldsymbol{\rho}_i, z)$. The positions of the optical vortices are determined through the equation set below:[36]

$$\begin{cases} \mathrm{Re}\left[\mu(\boldsymbol{\rho}_1,\boldsymbol{\rho}_2,z)\right] = 0, \\ \mathrm{Im}\left[\mu(\boldsymbol{\rho}_1,\boldsymbol{\rho}_2,z)\right] = 0, \end{cases} \tag{18}$$

where Re and Im denote the real and imaginary parts, respectively.

3. Interaction of two noncanonical optical vortices with opposite topological charge signs propagating through turbulent atmosphere

3.1. Case of equal topological charge magnitudes

Figure 3 illustrates the phase distributions of the spectral degree of coherence for a Gaussian beam carrying two noncanonical optical vortices after propagating through turbulent atmosphere over certain distances. The calculation parameters are $\lambda = 1.06$ μm, $w_0 = 3$ cm, $a = -2$, $c = 2$, $b = 1$ cm, $d = 1$ cm, $n = 1$, $m = 1$ (a)–(d), $n = 2$, $m = 2$ (e)–(h), $n = 3$, $m = 3$ (i)–(l), $\boldsymbol{\rho}_1 = (2\text{ cm}, 2\text{ cm})$, and $C_n^2 = 10^{-15}$ m$^{-2/3}$. As shown in Figs. 3(a)–3(d), at the source plane, the Gaussian

beam carries two noncanonical optical vortices with topological charges of $+1$ and -1, respectively. As the propagation distance increases to $z = 0.2$ km and $z = 0.6$ km, both vortices remain present, though their spatial positions change. When the propagation distance reaches $z = 2$ km, the optical vortices are no longer observed, indicating that annihilation has occurred at a certain propagation distance. From Figs. 3(e)–3(h), two noncanonical optical vortices with topological charges of $+2$ and -2 are present at the source plane. At $z = 0.2$ km, each of these optical vortices has evolved into two vortices with topological charges of $+1$ or -1. At $z = 0.6$ km, one pair of optical vortices with topological charges of $+1$ and -1 has annihilated, leaving two optical vortices remaining. At $z = 2$ km, two optical vortices with topological charges of $+1$ and -1 still exist. Figures 3(i)–3(l) show that for a Gaussian beam carrying two noncanonical optical vortices with topological charges of $+3$ and -3, the optical vortices at the source plane evolve into three optical vortices with topological charges of $+1$ and three with topological charges of -1 during propagation in turbulent atmosphere. As the propagation distance increases, two optical vortices with topological charges of $+1$ and two with topological charges of -1 annihilate due to the effects of turbulence, leaving only two optical vortices with topological charges of $+1$ and -1.

Therefore, Fig. 3 demonstrates that when a Gaussian beam carrying two noncanonical optical vortices with opposite topological charge signs propagates through turbulent atmosphere: when $m = n = 1$, the two optical vortices annihilate as the propagation distance increases; when $m = n > 1$, the two optical vortices evolve into $m + n$ optical vortices with topological charge magnitudes of 1 as the propagation distance increases, and with further propagation, annihilation occurs, and at sufficiently long distances, two optical vortices with topological charges of $+1$ and -1 remain on the wavefront.

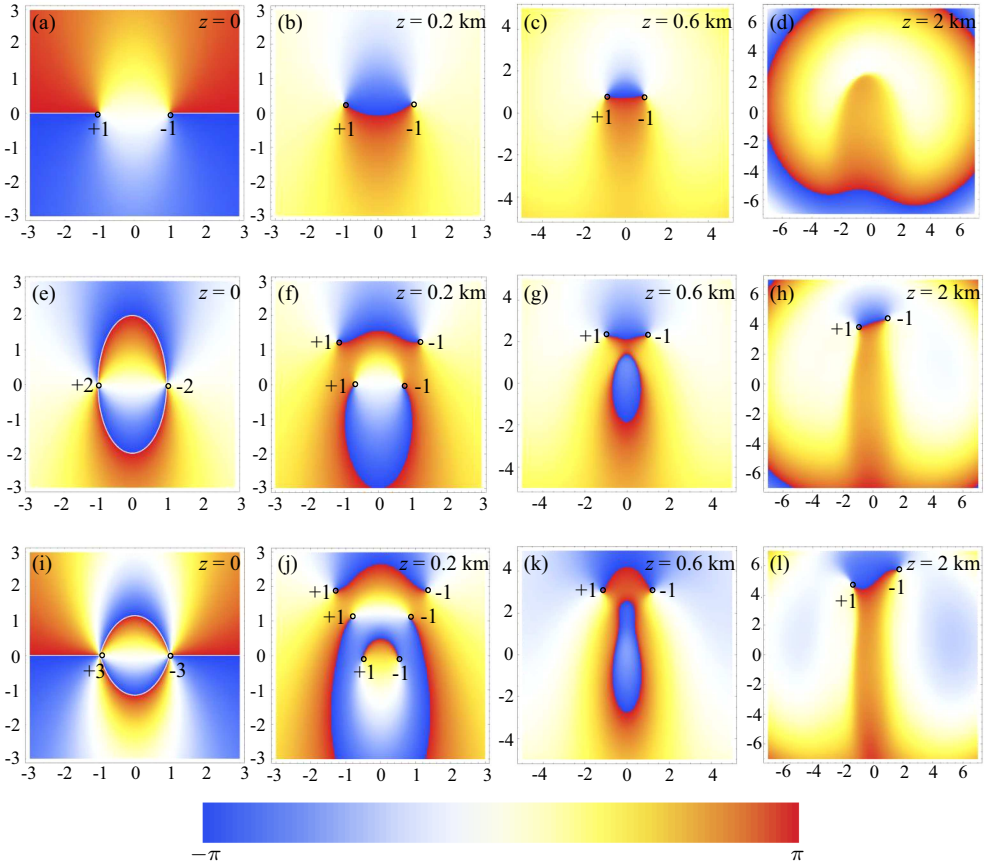


Fig. 3. Phase distributions of the spectral degree of coherence for a Gaussian beam carrying two noncanonical optical vortices after propagating through turbulent atmosphere at certain distances. The abscissa and ordinate represent ρ_{2x} and ρ_{2y}, respectively, in units of cm. $n = 1$, $m = 1$ (a)–(d), $n = 2$, $m = 2$ (e)–(h), and $n = 3$, $m = 3$ (i)–(l).

3.2. Case of unequal topological charge magnitudes

Figure 4 shows the phase distributions of the spectral degree of coherence for a Gaussian beam carrying two noncanonical optical vortices propagating through turbulent atmosphere. The calculation parameters are $n = 1$, $m = 2$ (a)–(d), $n = 1$, $m = 3$ (e)–(h), $n = 2$, $m = 3$ (i)–(l), and $n = 2$, $m = 4$ (m)–(p), with other parameters identical to those in Fig. 3. As shown in Figs. 4(a)–4(d), when a Gaussian beam carries a noncanonical optical vortex with a topological charge of -1 and another with $+2$, during propagation through turbulent atmosphere, the noncanonical optical vortex with a topological charge of $+2$ evolves into two optical vortices with topological charges of $+1$ at $z = 0.2$ km, while the optical vortex with a topological charge of -1 remains. At $z = 0.6$ km and

$z = 2$ km, the three vortices still exist. From Figs. 4(e)–4(h), when the two noncanonical vortices carried by the Gaussian beam have topological charges of -1 and $+3$, the optical vortex with a topological charge of $+3$ evolves into three optical vortices with topological charges of $+1$ as the propagation distance increases, while the position of the optical vortex with a topological charge of -1 shifts. As propagation continues, four vortices persist across the beam wavefront. As shown in Figs. 4(i)–4(l) and 4(m)–4(p), when the Gaussian beam carries two noncanonical vortices with topological charges of -2 and $+3$, or -2 and $+4$, respectively, both noncanonical optical vortices evolve into multiple optical vortices with topological charge magnitudes of 1 at $z = 0.2$ km during propagation through turbulent atmosphere, conserving total topological charge in the process. At $z = 0.6$ km, an optical vortex with a topological charge of -1 and an optical vortex with a topological charge of $+1$ on the wavefront have undergone annihilation, while the remaining optical vortices persist. At $z = 2$ km, the optical vortices present at $z = 0.6$ km still exist.

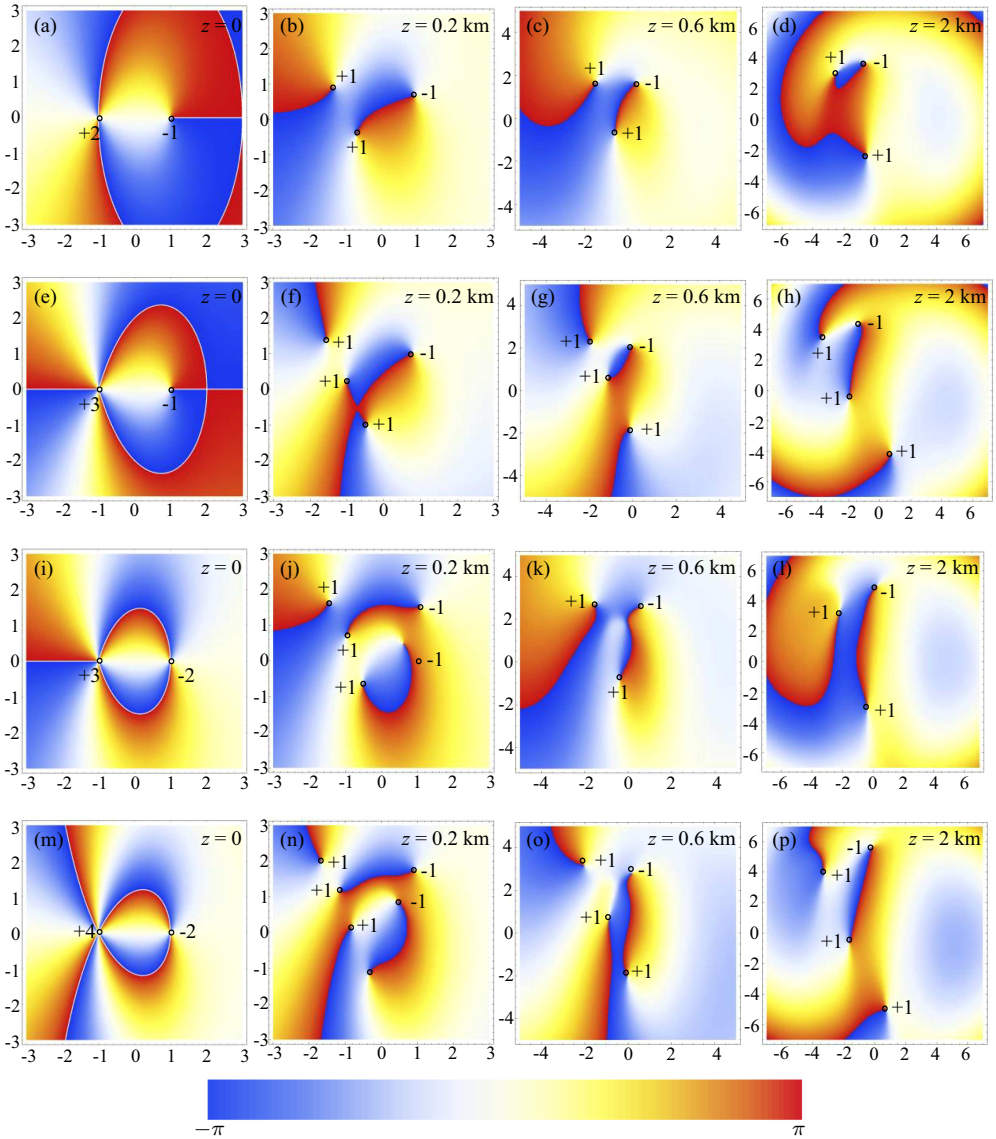


Fig. 4. Phase distributions of the spectral degree of coherence for a Gaussian beam carrying two noncanonical optical vortices propagating through turbulent atmosphere. The abscissa and ordinate represent ρ_{2x} and ρ_{2y}, respectively, in units of cm. $n = 1$, $m = 2$ (a)–(d), $n = 1$, $m = 3$ (e)–(h), $n = 2$, $m = 3$ (i)–(l), and $n = 2$, $m = 4$ (m)–(p).

Therefore, as shown in Fig. 4, when a Gaussian beam carrying two noncanonical optical vortices propagates through turbulent atmosphere and the two optical vortices have unequal magnitudes and opposite signs of topological charges, the following phenomena are observed: when the smaller of the two topological charge magnitudes equals 1, the optical vortex with a topological charge magnitude greater than 1 evolves into multiple optical vortices — each with a topological charge magnitude of 1 — as the propagation distance increases; with further propagation, these optical vortices on the wavefront remain stable. When the smaller topological charge magnitude of the two optical vortices is greater than 1, both optical vortices evolve into multiple optical vortices with topological charge magnitudes of 1 as the propagation distance in-

creases. With continued propagation, an optical vortex with a topological charge of -1 and another with $+1$ undergo annihilation, while the remaining optical vortices remain stable. In addition, when the two noncanonical optical vortices have unequal magnitudes and opposite signs of topological charges, the total topological charge remains conserved during propagation.

4. Interaction of two canonical optical vortices with opposite topological charge signs propagating through turbulent atmosphere

4.1. Case of equal topological charge magnitudes

Figure 5 illustrates the phase distributions of the spectral degree of coherence for a Gaussian beam carrying two canonical optical vortices after propagating through turbulent atmosphere over certain distances. The calculation parameters are $a = -1$, $c = 1$, $n = 1$, $m = 1$ (a)–(d), $n = 2$, $m = 2$ (e)–(h), and $n = 3$, $m = 3$ (i)–(l), with other parameters identical to those in Fig. 3. As shown in Figs. 5(a)–5(d), when the Gaussian beam carries one canonical optical vortex with a topological charge of -1 and another with $+1$, the two optical vortices undergo annihilation as the propagation distance increases due to the influence of atmospheric turbulence. According to Figs. 5(e)–5(h), when the Gaussian beam carries one canonical optical vortex with a topological charge of -2 and another with $+2$, during propagation through turbulent atmosphere, the optical vortex with a topological charge of -2 evolves into two optical vortices with topological charges of -1, while the optical vortex with a topological charge of $+2$ evolves into two optical vortices with topological charges of $+1$. As the propagation distance increases, one pair of optical vortices with topological charges of $+1$ and -1 annihilates first, followed by annihilation of the remaining pair. As shown in Figs. 5(i)–5(l), when the Gaussian beam carries canonical optical vortices with topological charges of -3 and $+3$ during propagation through turbulent atmosphere: at $z = 0.2$ km, the optical vortex with a topological charge of -3 and the optical vortex with a topological charge of $+3$ have respectively evolved into three optical vortices with topological charges of -1 and three with topological charges of $+1$; at $z = 0.6$ km, only one optical vortex with a topological charge of $+1$ and one optical vortex with a topological charge of -1 remain on the wavefront, while the other optical vortices have already undergone annihilation; at $z = 2$ km, no optical vortices remain on the wavefront, indicating that the optical vortices present at $z = 0.6$ km have also annihilated.

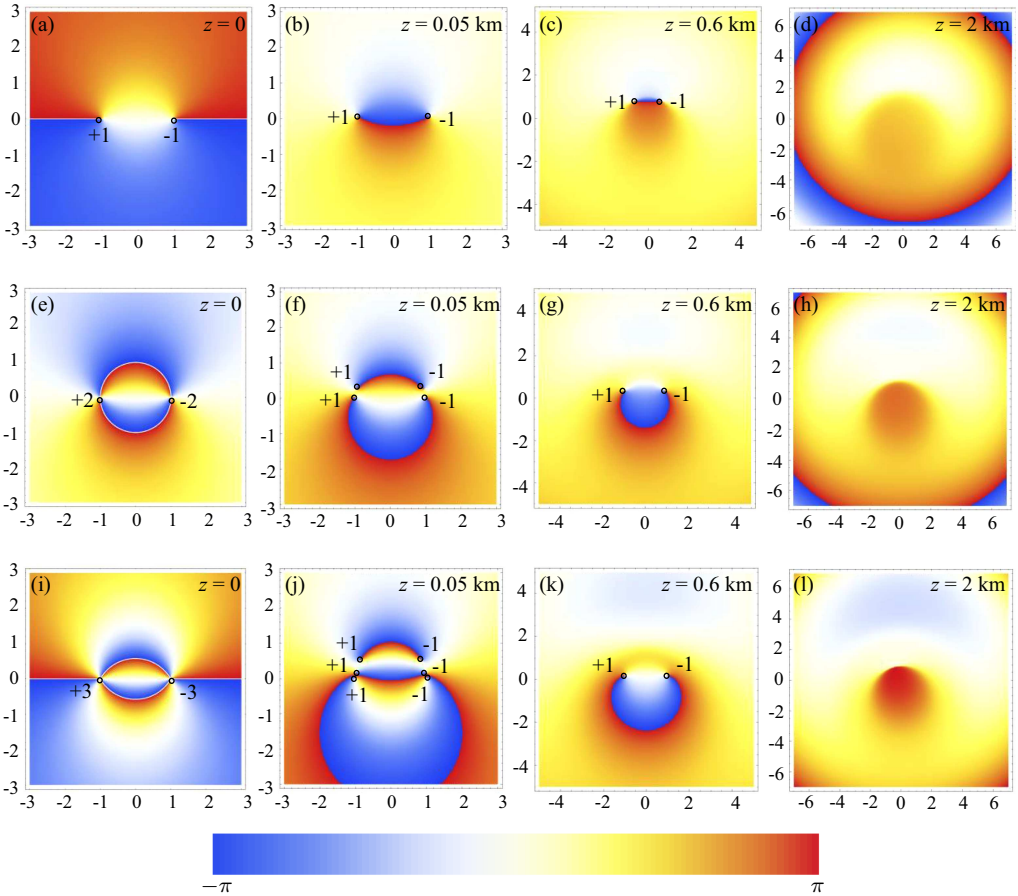


Fig. 5. Phase distributions of the spectral degree of coherence for a Gaussian beam carrying two canonical optical vortices after propagating through turbulent atmosphere at certain distances. The abscissa and ordinate represent ρ_{2x} and ρ_{2y}, respectively, in units of cm. $n = 1$, $m = 1$ (a)–(d), $n = 2$, $m = 2$ (e)–(h), and $n = 3$, $m = 3$ (i)–(l).

4.2. Case of unequal topological charge magnitudes

Figure 6 shows the phase distributions of the spectral degree of coherence for a Gaussian beam carrying two canonical optical vortices propagating through turbulent atmosphere. The calculation parameters are $n = 1$, $m = 3$ (a)–(d), $n = 2$, $m = 3$ (e)–(h), with other parameters identical to those in Fig. 5. As shown in Fig. 6, when the Gaussian beam carries two canonical optical vortices with topological charges of $+3$ and -1 or $+3$ and -2 during propagation through turbulent atmosphere, as the propagation distance increases, the optical vortex with a topological charge magnitude greater than 1 eventually evolves into multiple optical vortices each having a topological charge magnitude of 1, while the total topological charge remains conserved throughout this evolution. When the beam propagates over a sufficiently long distance, the number of optical vortices with topological charge magnitudes of 1 remaining on the wavefront equals the absolute value of the difference between the topological charges of the two initial optical vortices.

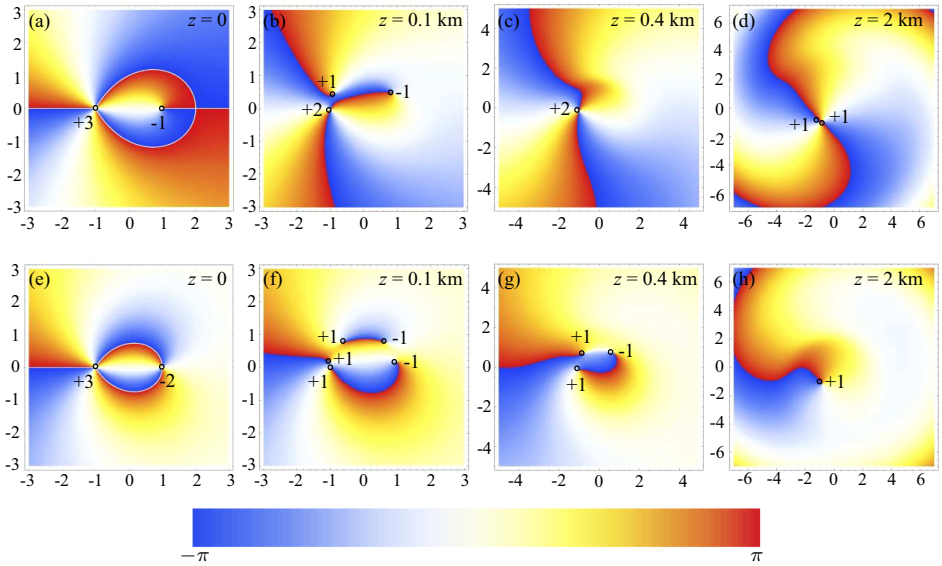


Fig. 6. Phase distributions of the spectral degree of coherence for a Gaussian beam carrying two canonical optical vortices propagating through turbulent atmosphere. The abscissa and ordinate represent ρ_{2x} and ρ_{2y}, respectively, in units of cm. $n = 1$, $m = 3$ (a)–(d), $n = 2$, $m = 3$ (e)–(h).

5. Interaction of two optical vortices with identical topological charge signs propagating through turbulent atmosphere

Figure 7 illustrates the phase distributions of the spectral degree of coherence for a Gaussian beam carrying two optical vortices after propagating through turbulent atmosphere over certain distances. The calculation parameters are $a = 1$, $c = 1$, $n = 2$, $m = 3$ (a)–(d), $a = 2$, $c = 2$, $n = 2$, $m = 3$ (e)–(h), with other parameters identical to those in Fig. 3. As shown in

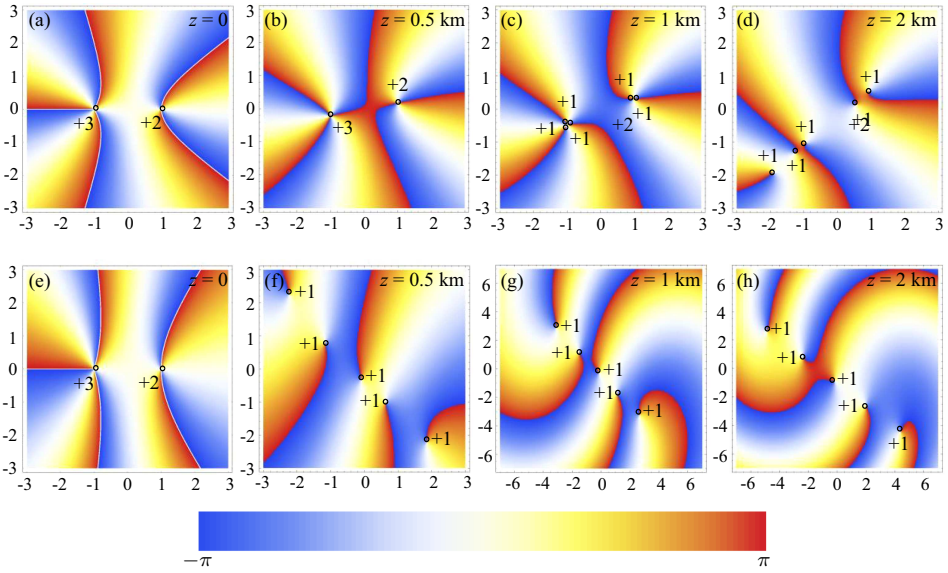


Fig. 7. Phase distributions of the spectral degree of coherence for a Gaussian beam carrying two optical vortices propagating through turbulent atmosphere. The abscissa and ordinate represent ρ_{2x} and ρ_{2y}, respectively, in units of cm. $a = 1$, $c = 1$, $n = 2$, $m = 3$ (a)–(d), $a = 2$, $c = 2$, $n = 2$, $m = 3$ (e)–(h).

Fig. 7, when a Gaussian beam carries two optical vortices with identical topological charge signs — regardless of whether they are canonical or noncanonical optical vortices — the two optical vortices evolve into multiple vortices with topological charge magnitudes of 1 as the propagation distance increases. The distances between these vortices gradually increase with further propagation. In addition, for two optical vortices with identical topological charge signs, the total topological charge remains conserved during propagation through turbulent atmosphere.

6. Conclusion

Based on the generalized Huygens–Fresnel principle, an analytical expression for the cross-spectral density function of a Gaussian beam carrying two optical vortices propagating through turbulent atmosphere was derived to study the interaction between the two optical vortices during propagation. First, the field expression of the Gaussian beam carrying two optical vortices at the source plane was given, and the phase distribution at the source plane was analyzed. It was found that for the dimensionless parameters a or $c = \pm 1$, the optical vortex exhibits a linear phase increase, characteristic of a canonical vortex, whereas for a or $c = \pm 2$, the nonlinear phase increase indicates a noncanonical vortex. Subsequently, the interaction of two optical vortices with opposite topological charge signs during propagation in turbulent atmosphere was investigated. The results show that when the two optical vortices have equal topological charge magnitudes ($m = n$) and $m > 1$, no optical vortices or only two optical vortices with topological charges of $+1$ and -1 remain on the beam wavefront after sufficiently long propagation. When the two optical vortices have unequal topological charge magnitudes ($m \neq n$) and the smaller one equals 1, there exist $m + n$ or $|m - n|$ optical vortices with topological charge magnitudes of 1 on the wavefront after sufficiently long propagation. Finally, the case of two optical vortices with identical topological charge signs was analyzed, revealing that as the propagation distance increases, both optical vortices evolve into multiple vortices, each with a topological charge magnitude of 1. Further, the total topological charge of a Gaussian beam carrying two optical vortices remains conserved during propagation through turbulent atmosphere. Besides, we numerically simulate the evolution behavior of two optical vortices in different atmospheric turbulence strengths, and find that the conclusion is still valid. The evolution difference between canonical and noncanonical optical vortices is due to the fact that the OAM modes carried by the beam itself are disturbed by atmospheric turbulence, and the energy of the OAM modes is redistributed. The findings of this study provide theoretical guidance for the application of optical vortices in optical communications.

Acknowledgements

Project supported by the Fundamental Research Program of Shanxi Province (Grant No. 202203021212169), the National Natural Science Foundation of China (Grant No. 62405230), and the Undergraduate Innovation and Entrepreneurship Training Program (Grant No. 2025DC32).

References

[1] Soskin M and Vasnetsov M 2001 *Prog. opt.* **42** 219
[2] Allen L, Beijersbergen M W, Spreeuw R and Woerdman J 1992 *Phys. Rev. A* **45** 8185
[3] Nye J F and Berry M V 1974 *Proc. R. Soc. Lond. A Math. Phys. Sci.* **336** 165
[4] Padgett M and Bowman R 2011 *Nat. Photonics* **5** 343
[5] Cojoc D, Garbin V, Ferrari E, Businaro L, Romanato F and Fabrizio E D 2005 *Microelectron. Eng.* **78–79** 125
[6] Willner A E, Song H, Zou K, Zhou H and Su X 2022 *J. Light. Technol.* **41** 1918
[7] Meng W, Li B, Luan H, Gu M and Fang X 2023 *ACS Photonics* **10** 2799
[8] Qiu S, Wang C, Liu T and Ren Y 2022 *Opt. Commun.* **524** 128767
[9] Almohamad S, Modler G K, Chutani R, Ghosh U U, Cleve S, Bruus H and Baudoin M 2025 *Phys. Rev. Appl.* **23** 054094
[10] Lu Z, Deng Y, Yu Y, Huang C and Yang J 2023 *Chin. Phys. Lett.* **40** 114201
[11] Zhu J, Wang L and Zhao S 2022 *IEEE Photon. Technol. Lett.* **35** 179
[12] Shi B, Ding D and Zhang W 2018 *J. Phys. B* **51** 032004
[13] Wang Q, Wang F, Liu J, Chen W, Han Z, Forbes A and Wang J 2021 *Phys. Rev. Appl.* **15** 064034
[14] Baliyan M and Nishchal N K 2024 *Opt. Lasers Eng.* **180** 108337
[15] Chen S, Chen J, Xia T, Xie Z, Huang Z, Zhou H, Liu J, Chen Y, Li Y and Yu S 2025 *Adv. Photon.* **7** 044001
[16] Zhang R, Cui X, Zeng Y, Chen J, Liu W, Wang M, Wang D, Zhang Z, Wang N and Wu G 2025 *Nature* **641** 1142
[17] Chen Q, Qu G, Yin J, Wang Y, Ji Z, Yang W, Wang Y, Yin Z, Song Q, Kivshar Y and Xiao S 2024 *Nat. Nanotechnol.* **19** 1000
[18] Jo J, Byun S, Bae M, Wang J, Chung H and Kim S 2025 *Light Sci. Appl.* **14** 277
[19] Peters C, Cocotos V and Forbes A 2025 *Adv. Opt. Photon.* **17** 113
[20] Li J, Liang H, Wu G, Peng P, Wang F and Cai Y 2025 *APL Photonics* **10** 016117
[21] Gao P, Lu M, Li J and Li J 2025 *Phys. Scr.* **100** 055525
[22] Saad F, Ebrahim A A A, Benzehoua H and Belafhal A 2025 *Opt. Quant. Electron.* **57** 171
[23] Bai Y, Zhu Y, Wang J, Li M, Khakhomov S and Hu Z 2024 *Opt. Express* **32** 23584
[24] Duan Q, Zhao P, Yin Y and Chen H 2024 *Chin. Phys. B* **33** 014202
[25] Gao P, Lu M and Li J 2023 *Opt. Continuum* **2** 2374
[26] Lyu Z, Wang P and Wang C 2023 *Chin. Phys. B* **32** 124209
[27] Freund I and Shvartsman N 1994 *Phys. Rev. A* **50** 5164
[28] Wang Y, Bai L, Xie J, Zhang D, Lv Q and Guo L 2021 *Opt. Express* **29** 16056
[29] Gao P and Bai L 2020 *OSA Continuum* **3** 2797
[30] Deng D and Guo Q 2010 *Appl. Phys. B* **100** 897
[31] Huang S, Miao Z, He C, Pang F, Li Y and Wang T 2016 *Opt. Lasers Eng.* **78** 132
[32] Gradshteyn I and Ryzhik R 2007 *Tables of Integrals, Series and Products* (New York: Acadenic Press) pp. 25–365
[33] Andrews L C and Phillips R L 2005 *Laser Beam Propagation Through Random Media* (Bellingham: SPIE Press) pp. 135–178
[34] Wang S C H and Plonus M A 1979 *J. Opt. Soc. Am.* **69** 1297
[35] Mandel L and Wolf E 1995 *Optical Coherence and Quantum Optics* (Cambridge: Cambridge University Press) pp. 147–228
[36] Gbur G and Visser T D 2003 *Opt. Commun.* **222** 117